In vitro evaluation of human osteoblast adhesion to a thermally oxidized γ-TiAl intermetallic alloy of composition Ti–48Al–2Cr–2Nb (at.%)

Samir A. Bello · Idaris de Jesús-Maldonado · Esteban Rosim-Fachini · Paul A. Sundaram · Nanette Diffoot-Carlo

Abstract Ti–48Al–2Cr–2Nb (at.%) (γ-TiAl), a gamma titanium aluminide alloy originally designed for aerospace applications, appears to have excellent potential as implant material. Thermal treatment of γ-TiAl renders this alloy extremely corrosion resistant in vitro, which could improve its biocompatibility. In this study, the surface oxides produced by thermal oxidation (at 500°C, and at 800°C for 1 h in air) on γ-TiAl were characterized by X-ray photoelectron spectroscopy (XPS). hFOB 1.19 cell adhesion on thermally oxidized γ-TiAl was examined in vitro by a hexosaminidase assay, scanning electron microscopy (SEM) and confocal laser scanning microscopy (CLSM) after 1, 7 and 14 days. Ti–6Al–4V surfaces were used for comparison. Hexosaminidase assay data and CLSM analysis of focal contacts and cytoskeleton organization showed no differences in cell attachment on autoclaved and both heat-treated γ-TiAl surfaces at the different time points. SEM images showed well organized multi-layers of differentiated cells adhered on thermally oxidized γ-TiAl surfaces at day 14. Unexpectedly, thermally oxidized Ti–6Al–4V surfaces oxidized at 800°C exhibited cytotoxic effects on hFOB 1.19 cells. Our results indicate that thermal oxidation of γ-TiAl seems to be a promising method to generate highly corrosion resistant and biocompatible surfaces for implant applications.

1 Introduction

Titanium (Ti) and its alloys have been used as implant materials due to their excellent biocompatibility. Although Ti–6Al–4V is the most common titanium alloy used in bone repair and replacement, its use as a biomaterial has some constraints. The possibility of vanadium (V) ion release, considered a toxic element [1], and the low wear resistance of Ti–6Al–4V are of serious concerns in using this alloy as a biomaterial [2, 3]. This has led to the study of different V-free Ti alloys as possible alternatives. Among the V-free Ti alloys investigated for potential biomedical applications are new generations of the γ-based TiAl intermetallic alloys, which originally were developed for aerospace and automotive applications. γ-TiAl alloys possess low density (3.8 g/cm^3), high stiffness and mechanical strength (up to 1,000 MPa), and good oxidation and corrosion properties [4, 5]. Recently, the biocompatibility of Ti–48Al–2Cr–2Nb (at.%) (hereafter referred to as γ-TiAl), a second generation γ-titanium aluminide, has been demonstrated in vitro [6] and in vivo [7].

Biocompatibility of titanium and its alloys is mainly due to the reactive oxide layer, typically 4–6 nm thick, which spontaneously forms at room temperature. This surface oxide layer or passive layer (amorphous or poorly crystallized TiO$_2$) confers high stability, chemical inertness, and a high in vitro corrosion resistance in many oxidizing media [8]. However, when the titanium alloy is implanted in vivo, in a physiologically aggressive environment, the oxide stability may be altered resulting in increased metal

S. A. Bello · I. de Jesús-Maldonado · N. Diffoot-Carlo (✉)
Department of Biology, University of Puerto Rico, Call Box 9000, Mayagüez Campus, Mayagüez, PR 00681-9000, USA
e-mail: nanette.diffoot@upr.edu

E. Rosim-Fachini
Department of Physical Sciences, General Studies Faculty, University of Puerto Rico, P.O. Box 23346, Río Piedras Campus, San Juan, PR 00931, USA

P. A. Sundaram
Department of Mechanical Engineering, University of Puerto Rico, Call Box 9000, Mayagüez Campus, Mayagüez, PR 00680, USA

ion release and implant failure [9]. Furthermore, in vitro studies have shown that ions associated with Ti–6Al–4V alloy inhibited the normal differentiation of bone marrow stromal cells to mature osteoblasts, suggesting that the metal ion release from Ti–6Al–4V may inhibit the bone formation on implant surfaces [10]. Particulate and ionic debris resulting from in vivo degradation of total joint replacement components are recognized as major factors limiting the longevity of the joint reconstruction [11].

Surface treatment modalities of titanium alloys, including thermal oxidation, have been tested as methods to modify the surface oxide composition and thickness of Ti alloys, thus improving its wear and corrosion resistance [9]. Thermal oxidation is a cheap and easy way to originate thick and highly crystalline ceramic coatings on Ti alloys, which provide good protection and reduce the friction coefficients in rubbing contact. Pre-clinical evidences indicate that bone-to-implant contact is significantly higher on thermally oxidized oral Ti implants compared to conventional oral Ti implants, suggesting that thermal oxidation could improve the osseointegration [12]. In vitro studies have established that thermal oxidation increases the corrosion resistance of γ-titanium aluminides [4, 5] and Ti–6Al–4V alloys [3, 8, 13–15]. Furthermore, some studies have reported increased osteoblast adhesion on thermally oxidized Ti–6Al–4V surfaces [3, 14, 15].

There is currently no information available related to the response of osteoblast cells to thermally oxidized γ-TiAl surfaces. Our hypothesis is that thermally oxidized γ-TiAl surfaces display similar or improved biocompatibility compared to autoclaved γ-TiAl surfaces, using as an indicator of biocompatibility the cell adhesion capability on the different surfaces. In this work the adhesion of hFOB 1.19 osteoblasts on thermally oxidized (at 500 and 800°C for 1 h in air) γ-TiAl surfaces was evaluated in vitro by a hexosaminidase assay, scanning electron microscopy (SEM) and immunofluorescent labeling of vinculin and F-actin. This study will have a strong impact in determining the biocompatibility and potential usefulness of thermally oxidized γ-TiAl as a biomaterial. For comparison purposes, thermally oxidized Ti–6Al–4V surfaces were also investigated.

2 Materials and methods

2.1 Preparation of disks

γ-TiAl [Ti–48Al–2Cr–2Nb (at.%)] disks of both 5 and 9 mm in diameter and thickness of 1 mm were manually cut from γ-TiAl rods using a low speed saw (Buehler™). The surfaces were prepared manually in an Ecomet 3 (Buehler™) by wet grinding with 600 grit silicon carbide paper, and they were ultrasonically cleaned in 0.8% Alconox (Fisher) and

95% ethanol for 10 min each, while rinsing with deionized water between each cleaning process. The disks were dried and then oxidized in a laboratory furnace (CM Furnaces Inc.) in air at 500°C or at 800°C for 1 h. They were then transported aseptically to the cell culture laboratory and placed in 48-well cell culture plates (Corning). γ-TiAl disks polished and cleaned as described previously, and subsequently sterilized by autoclaving (121°C, 15 psi, 15 min) were used as controls. Ti–6Al–4V alloy disks manually cut from machined wrought ($\alpha + \beta$) annealed rods and oxidized at 500 or 800°C and sterilized by autoclaving were processed as described for γ-TiAl disks and used for comparison purposes. Autoclaved, thermally oxidized at 500 and 800°C γ-TiAl and Ti–6Al–4V disks will be referred hereafter as GTi, TiV, GTi5, TiV5, GTi8 and TiV8, respectively.

2.2 Surface characterization of disks

X-ray photoelectron spectroscopy (XPS) was performed on samples in a PHI 5600 Multisystem Electron Spectrometer, equipped with a monochromatic Al source and a neutralizer. The base pressure was 1×10^{-9} Torr or higher. A survey spectrum in the 0–1,100 eV window for binding energy was obtained for each sample using pass energy of 187.85 eV, in order to verify the major components and possible contaminants. Narrow binding energy windows for high resolution scans were obtained for peaks of interest using pass energy of 58.70 eV. All peak positions were corrected taking into account C1s for adventitious species at 284.8 eV. The peak deconvolution and data analyses were performed using the software Multipak v. 6.0A (Physical Electronics Inc.).

2.3 Cell line

Human osteoblast cell line hFOB 1.19 (CRL-11372) (ATCC) were cultured in 90% Dulbecco's Modified Eagle's Medium Nutrient Mixture F-12 Ham (DMEM) (Sigma-Aldrich) with 2.5 mM L-glutamine and 15 mM hepes, without phenol red, supplemented with 0.3 mg/ml G-418 (Calbiochem) and 10% fetal bovine serum (FBS) (Hyclone). Cells were grown in 25 cm^2 plastic culture flasks (Corning) and incubated at 33.5°C until subconfluence. At approximately 90% confluence, cells were washed three times with phosphate buffered saline (PBS) and harvested using 0.25% trypsin–0.53 mM EDTA (Gibco) at 37°C for 5 min. Cells were pelleted by low-speed centrifugation (3,800 rpm) for 5 min, and subcultured in a 1:3 ratio.

2.4 Hexosaminidase assay

hFOB 1.19 cells were seeded at a density of 5×10^4 cells/cm^2 on all the disks tested (5 mm diameter) and were

incubated for 24 h (1 day) and 7 days at 33.5°C, and 14 days (7 days at 33.5°C, and then for 7 days at 39.5°C) in serum containing media. Cells cultured on polystyrene were used as cell growth controls. After incubation, the samples were gently rinsed three times in PBS to remove the unattached cells, and the disks were then transferred to a 96-well tissue culture plate (Becton Dickinson) where the number of attached cells was quantified by the hexosaminidase assay as described previously [3, 16], using the β-N-Acetylglucosaminidase Assay Kit (Sigma-Aldrich). Three independent experiments were performed, with each experiment performed in triplicate. A standard curve of hexosaminidase activity versus cell number measured by a Neubauer chamber was run for every experiment [3].

2.5 Scanning electron microscopy analysis

hFOB 1.19 cells were seeded at a density of 5×10^4 cells/ cm^2 on all the surfaces tested (9 mm in diameter) and were incubated for 14 days (7 days at 33.5°C, and then for 7 days at 39.5°C) in serum containing media. Disks incubated with culture media but without cells were used as negative controls. Cells growing on glass coverslips were used as cell growth controls. After incubation, samples were washed carefully with PBS and fixed overnight in 4% glutaraldehyde buffered in PBS at 4°C. After washing three times with PBS, the samples were dehydrated in graded ethanol (10–100%) for 10 min each. After critical point drying (EMS 850) samples were mounted on stubs and were sputtered coated with gold (EMS 550X). Samples were then examined with a JEOL JSM-5410 LV SEM (JEOL, Japan) at 10 or 15 kV using variable magnifications ($1,500\times$ and $5,000\times$). Two independent experiments in triplicate were carried out.

2.6 Immunofluorescent staining of actin cytoskeleton and focal contacts

hFOB 1.19 cells were seeded at a density of 1.5×10^4 cells/cm^2 on all the test samples (9 mm diameter) and were incubated for 1 and 7 days at 33.5°C, and 14 days (7 days at 33.5°C, and then for 7 days at 39.5°C) in serum containing media. After incubation, cells were fixed using 4% formaldehyde [at room temperature (RT), 15 min] and washed with wash buffer (PBS containing 0.05% Tween-20). Cells were permeabilized with 0.1% Triton X-100 (5 min, RT), and blocked using blocking solution [1% BSA and 5% normal goat serum in PBS] for 30 min at RT. F-actin, vinculin and cell nuclei were stained using a commercial kit (Chemicon), and visualized as red, green, and blue fluorescence, respectively. After blocking, samples were incubated (1 h, RT) with anti-vinculin monoclonal antibody (1:200), washed followed by

incubation (1 h, RT in the dark) with AlexaFluor® 647-labeled secondary goat anti-mouse immunoglobulin G (1:200, Molecular Probes) and TRITC-conjugated phalloidin (1:200, Chemicon). Samples were washed again and then cell nuclei were contrast-labeled in blue by incubation (5 min, RT in the dark) with 0.1 μg/ml DAPI followed by washing. Samples were mounted in 24×60 mm coverslips with ProLong™ Gold antifade reagent (Invitrogen) and stored at 4°C in the dark. Finally, samples were observed using an inverted confocal laser scanning microscope (FluoView™ 300, Olympus, USA) equipped with 405LD, 543 Green HeNe, and 633 Red HeNe lasers, and a $60\times/1.4$ oil immersion objective. Cells growing on glass coverslips were used for positive and negative controls.

2.7 Statistical analysis

Hexosaminidase assay data were analyzed using a factorial ANOVA. All factors were considered fixed. Post hoc comparisons were analyzed by multiple contrasts of hypotheses using 95% Bonferroni intervals of confidence when interactions were found. Otherwise, one-way ANOVAs and Tukey tests were performed. The P values ≤0.05 were considered to be statistically significant. All analyses were performed using Minitab® 14 (Minitab Inc.).

3 Results

3.1 Surface characterization of disks

Representative wide-scan XPS spectra of the thermally oxidized γ-TiAl and Ti–6Al–4V surfaces are shown in Fig. 1 and their corresponding surface atomic compositions are given in Table 1. The observed metal ratio on the polished and autoclaved γ-TiAl and Ti–6Al–4V surfaces indicated that γ-TiAl surfaces were enriched in Cr and deficient in Ti whereas Ti–6Al–4V were enriched in Al and deficient in Ti relative to the bulk alloys.

Deconvolution treatment of XPS envelopes for Al 2p, Ti 2p, and O 1s transitions are presented in Fig. 2. The XPS spectra from the polished and autoclaved γ-TiAl (Fig. 2b) and also for Ti–6Al–4V (data not shown) surfaces exhibited a weak signal for Ti $2p_{3/2}$ at 453.5 eV, which can be assigned to metallic titanium, and an intermediate oxide form, assigned to Ti^{3+} at 456.7 eV, which may correspond to Ti_2O_3 (Fig. 2b). Both γ-TiAl and Ti–6Al–4V surfaces thermally oxidized at 500 and 800°C exhibited a Ti^{4+} form at 458.6 eV, which can be assigned to TiO_2 (Fig. 2b).

The center of the Al 2p peak of polished, autoclaved, and thermally oxidized γ-TiAl (Fig. 2a) and Ti–6Al–4V (data not shown) layers was located at 74 eV, indicating
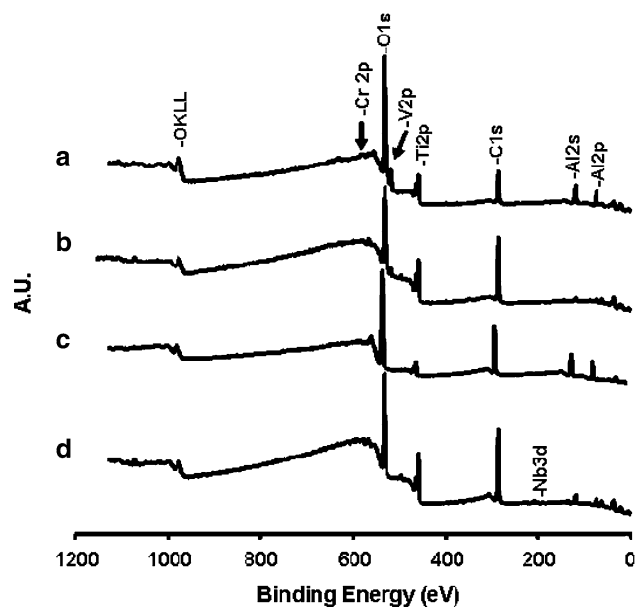
Fig. 1 Representative wide-scan XPS spectra of thermally oxidized at 500°C (**b**, **d**) and at 800°C (**a**, **c**) for γ-TiAl (**c**, **d**) and Ti–6Al–4V (**a**, **b**) surfaces

the formation of Al_2O_3 on all samples. However, metallic aluminum was also evident by the peak at 71.4 eV on polished and autoclaved γ-TiAl (Fig. 2a) and Ti–6Al–4V (data not shown) layers. Deconvolution of O 1s envelope showed three different peaks at 533, 531.5, and 530 eV, which may correspond to water, hydroxides and oxygen from organic matrix and oxides, respectively, on all γ-TiAl (Fig. 2c) and Ti–6Al–4V surfaces (Fig. 2d).

Examples for the weak peaks observed in the XPS spectra corresponding to Nb 3d, P 2p, Cr 2p, V 2p, and Cr 2p are presented in Fig. 2e. The center for the Nb 3d on polished, autoclaved and thermally oxidized γ-TiAl layers was located at 207.0 eV, indicating the formation of a Nb^{5+} oxide, probably in the form of Nb_2O_5 or some oxo-hydroxide species. On these samples, a peak located at 577.6 eV indicated the formation of a Cr^{3+} oxide, probably

in the form of Cr_2O_3. On the polished, autoclaved and thermally oxidized Ti–6Al–4V samples, the doublet V 2p$_{3/2,1/2}$ at 516.4 and 524.0 eV were observed, which may correspond to an oxo-hydroxide form of V^{5+} or V^{4+} for V_2O_5 or VO_2 [3, 17, 18], respectively.

While a slight decrease in the minor metal components (Cr for γ-TiAl, and V for Ti–6Al–4V) on the surfaces which were thermally oxidized at 500°C was observed, an increase in these same components was observed for surfaces which were thermally oxidized at 800°C (Fig. 3). The Cr/Ti and V/Ti ratios on γ-TiAl and Ti–6Al–4V surfaces thermally oxidized at 800°C, respectively, were higher than the same ratios on γ-TiAl and Ti–6Al–4V surfaces thermally oxidized at 500°C (Fig. 3), suggesting that oxidation at 800°C causes an enrichment of Cr and V oxides on γ-TiAl and Ti–6Al–4V surfaces, respectively.

3.2 Hexosaminidase assay

The estimated average number and standard deviation (SD) of osteoblast cells attached on the different surfaces at each time point are shown in Fig. 4a. The interaction between type of metal (γ-TiAl or Ti–6Al–4V), incubation period (1, 7, or 14 days) and the temperature of oxidation (121, 500, or 800°C) yielded significant differences ($P \leq 0.05$). There were no significant differences in cell attachment among the six surfaces studied after 1 day of incubation. In contrast, the number of osteoblast cells attached to TiV8 surfaces was significantly less compared to the other surfaces tested at both 7 and 14 days post-incubation (Fig. 4a).

The factorial ANOVA carried out excluding the data of cell attachment on GTi8 and TiV8 showed that the interaction between the three factors (type of metal, time of incubation and temperature of oxidation) yielded no significant differences ($P > 0.05$). In addition, there were no significant differences in cell attachment among the four surfaces studied at the three time points tested (1, 7, and 14 days) (Fig. 4b). Cell attachment increased significantly

Table 1 Surface composition (at.%) of the polished (GTi-P, TiV-P), autoclaved (GTi, TiV), thermally oxidized at 500°C (GTi5, TiV5), and at 800°C (GTi8, TiV8) γ-TiAl and Ti–6Al–4V surfaces

Sample	%C	%O	%Al	%P	%Ti	%Cr	%Nb	%V	%Al/%Ti	%Cr/%Ti	%Nb/%Ti	%V/%Ti	%O/%M
GTi-P	57.2	30.3	5.6	0.7	4.6	1.3	0.2	N/A	1.2	0.3	0.0	N/A	2.6
GTi	55.4	31.7	5.9	0.8	4.9	1.0	0.2	N/A	1.2	0.2	0.0	N/A	2.6
GTi5	48.7	35.4	6.7	0.5	7.4	1.1	0.2	N/A	0.9	0.1	0.0	N/A	2.3
GTi8	39.7	37.4	19.2	0.0	1.8	2.0	0.0	N/A	10.8	1.1	0.0	N/A	1.6
TiV-P	52.3	34.6	2.4	0.9	9.6	N/A	N/A	0.2	0.3	N/A	N/A	0.0	2.8
TiV	52.7	35.2	1.8	0.4	9.7	N/A	N/A	0.2	0.2	N/A	N/A	0.0	3.0
TiV5	49.7	36.8	3.6	ND	8.6	N/A	N/A	1.3	0.4	N/A	N/A	0.1	2.7
TiV8	44.6	37.6	6.7	ND	9.3	N/A	N/A	1.8	0.7	N/A	N/A	0.2	2.1

ND not detected, *N/A* not apply

Fig. 2 Deconvolution of Al
2p$_{3/2}$ (**a**), Ti 2p$_{3/2,1/2}$ (**b**), and O
1s peaks for γ-TiAl alloy (**c**), O
1s peak for Ti–6Al–4V (**d**). The
results for polished (*OA*),
autoclaved (*OB*), oxidized at
500°C (*I*) and at 800°C (*II*) are
displayed. XPS spectra for
minor constituents of
autoclaved γ-TiAl and thermally
oxidized at 500°C Ti–6Al–4V
surfaces are shown in (**e**)
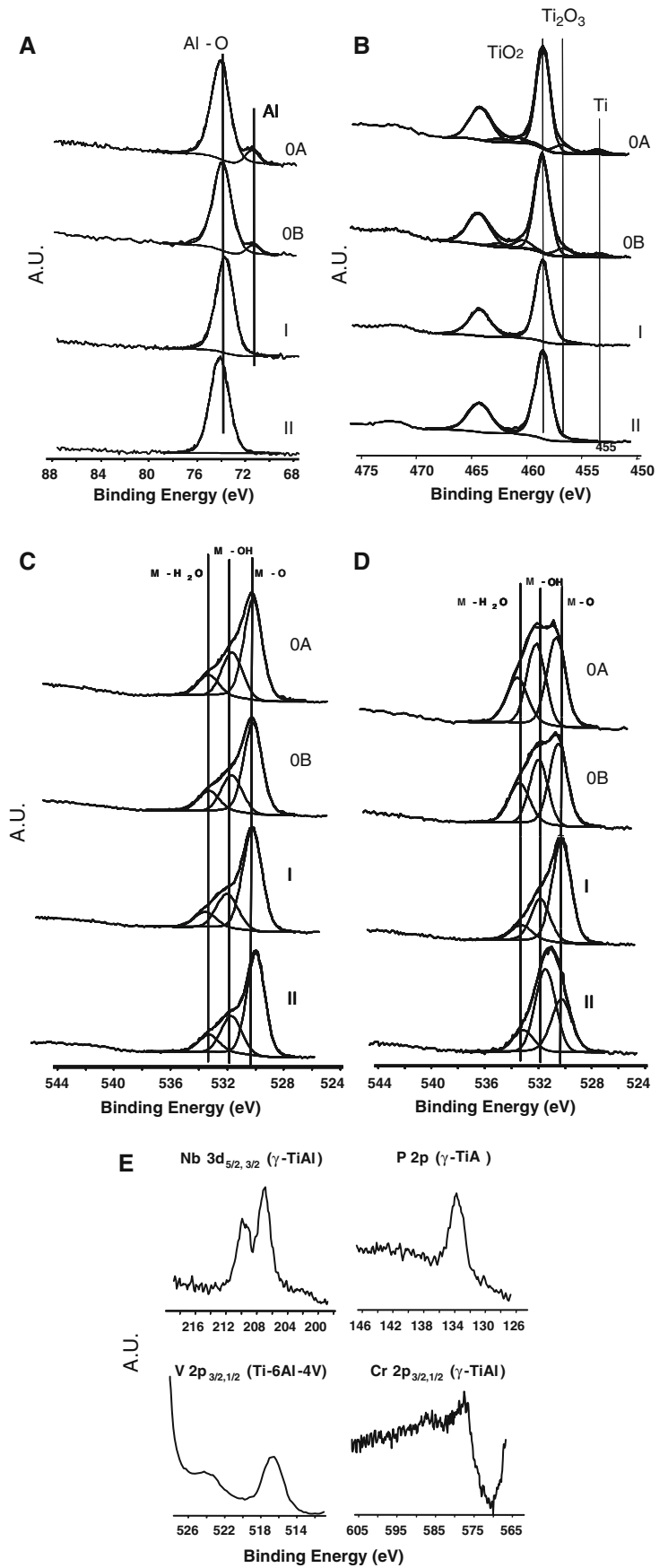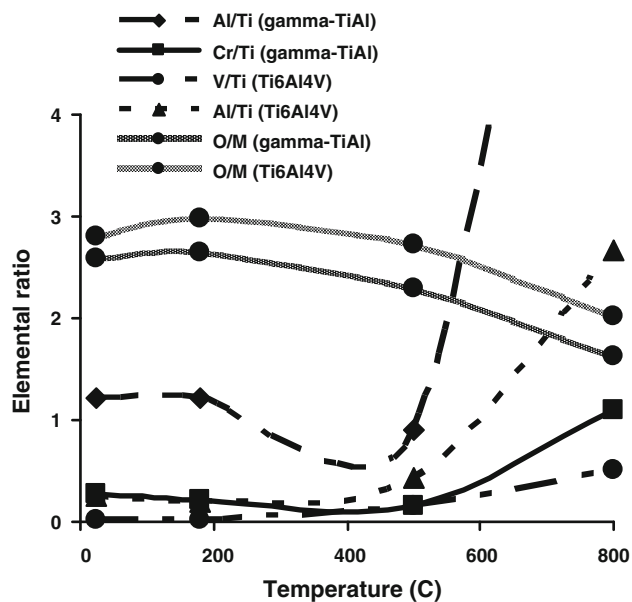
Fig. 3 Variability in the metal elemental ratio on γ-TiAl and Ti–6Al–4V surfaces from XPS data according to the temperature of oxidation

between days 1 and 7 on all tested surfaces ($P \leq 0.05$). After this time, the number of attached cells remained constant on all assessed surfaces (Fig. 4b).

3.3 Assessment of cell attachment by SEM

SEM images showed that hFOB 1.19 cells were attached on glass, all γ-TiAl disks, and on TiV and TiV5 disks, but they were not adhered on TiV8 disks after 14 days of incubation (Fig. 5a–n). The osteoblast cells formed multi-layered confluent cultures on all the surfaces, except on TiV8. On the TiV8 samples only a few scattered irregular structures were observed (Fig. 5n), resembling the appearance of the TiV8 negative control disk (Fig. 5t).

No morphological differences of hFOB 1.19 cells grown on all the surfaces, except on TiV8, were observed. Cells were mainly elongated and polygonal with many filopodia. Some cells exhibited numerous small sphere-like surface evaginations. Fibrous networks and rounded sponge-like structures of different sizes were present on all the surfaces tested, except on TiV8 surfaces (Fig. 5a–n).

The appearance of the negative control disks (incubated for 14 days without cells) is shown in Fig. 5o–t. Parallel grooves and striations generated by the grinding process were observed on all the surfaces, except on TiV8. GTi5 and TiV5 surfaces (Fig. 5p and s, respectively) looked very similar, exhibiting rounded to irregular structures different in size that probably correspond to oxide particles. GTi8 and TiV8 surfaces (Fig. 5q and t, respectively) appeared very granular but the oxide granules formed on TiV8 were bigger compared to the granules formed on GTi8,

conferring to TiV8 a rougher and more irregular appearance (Fig. 5t).

### 3.4 Immunofluorescent staining of actin cytoskeleton and focal contacts

Most cells exhibited an elongated or polygonal morphology and contained many stress fibers in a parallel arrangement on all but TiV8 surfaces at all time points (Figs. 6, 7). Cells were gradually spreading out over time. At day 14 cells appeared fully spread compared to cells at days 1 and 7. On TiV8 only rounded cells with many microspikes and no well-defined stress fibers were visible at day 1 (Fig. 7g). At day 7, cells on TiV8 were rounded and smaller compared to cells at day 1 and had also lost their cell projections and exhibited only cell nuclei remnants (Fig. 7h). At day 14 no cells were observed on TiV8 (Fig. 7i).

At day 1, a few focal adhesions were seen at the cell periphery on all the surfaces (Figs. 6g, 7d), except on TiV8. The number and size of focal adhesions appeared to increase from day 1 to 7 on all the surfaces, except on TiV8. At day 14, the relative number and size of focal contacts appeared to decrease on all surfaces, except on GTi, where they appeared to remain constant (Fig. 6c). The majority of the focal adhesions on all the surfaces were oriented in the same direction as the stress fibers. At days 1 and 7, diffuse perinuclear vinculin expression instead of defined focal adhesions was observed in cells on TiV8 (Fig. 7g, h). No cells were observed on TiV8 after 14 days of culture (Fig. 7i).

4 Discussion

Thermal oxidation is an easy and cost-effective surface treatment applied to Ti or its alloys to increase the corrosion resistance, which is a desirable characteristic of implant materials. However, there is not much agreement about the effects of thermal oxidation of Ti or its alloys on osteoblast cell adhesion. In this study, neither the quantitative data from the hexosaminidase assay nor the qualitative data from the SEM and the immunofluorescent detection of focal adhesions showed differences in the amount of cells adhered on any of the γ-TiAl surfaces evaluated (autoclaved and thermally oxidized at 500 or 800°C) at the different time points (1, 7, and 14 days). Results were similar on the autoclaved and thermally oxidized at 500°C Ti–6Al–4V surfaces. However, hFOB 1.19 cells displayed an unexpected behavior on Ti–6Al–4V oxidized at 800°C especially after 7 and 14 days of incubation.

Fig. 4 hFOB 1.19 cell attachment on autoclaved and thermally oxidized γ-TiAl and Ti–6Al–4V disks. Cells were cultured on GTi, GTi5, GTi8, TiV, TiV5, and TiV8 surfaces for 1, 7, and 14 days. The data are expressed as the number of cells attached on the different substrates (**a**), or the number of cells attached on GTi, GTi5, TiV, and TiV5 (not taking into account the data of cells attached on GTi8 and TiV8) (**b**) determined by the hexosaminidase assay. Each value represents the mean ± SD of three independent experiments, each performed in triplicate ($N = 9$). *$P \leq 0.05$ compared to all others surfaces tested, at the corresponding time point. [a]$P \leq 0.05$ compared to day 1
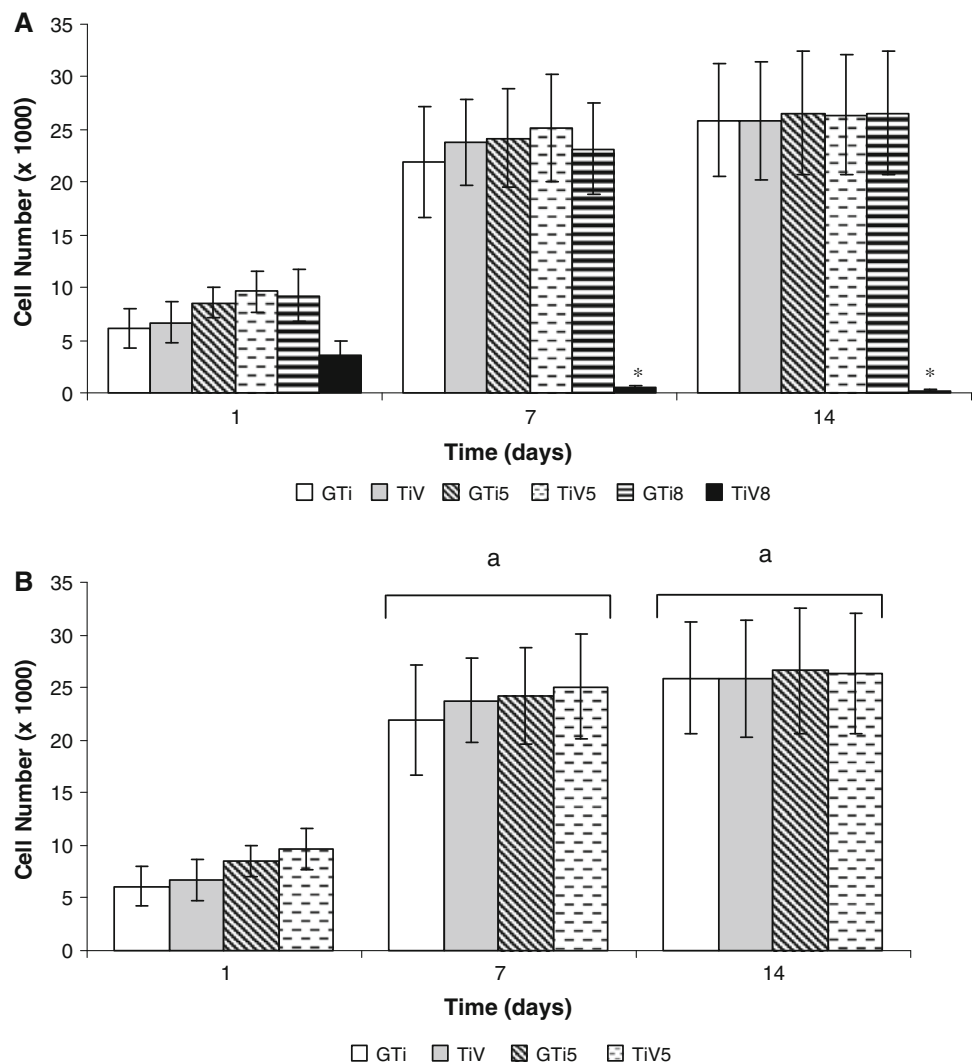

This research agrees with some studies that have reported no differences among cell attachment on control metallic surfaces (polished but not thermally oxidized) compared with the thermally oxidized surfaces [13, 19]. Other studies have reported increased cell adhesion on heat treated Ti or Ti alloys [3, 20] while some time-course cell adhesion experiments, have reported increased numbers of osteoblast cells attached on heat treated Ti or Ti alloys in all [21] or in some of the specific time points tested [14, 15].

Our XPS measurements indicated the formation of oxide scales composed of a mixture of TiO_2, Al_2O_3, Cr_2O_3, and Nb_2O_5 oxides on all the γ-TiAl surfaces. The absence of the peak at Ti 2p3/2 at 453.5 eV (metallic titanium) on thermally oxidized samples suggested that the oxide layer on these surfaces is thicker compared to native oxide layers, which agrees with literature [13, 14]. Additionally, it was found that oxidation at 800°C causes an enrichment of Cr and Al oxides on the γ-TiAl surfaces. However, the

increased amount of Al_2O_3 on the γ-TiAl surface oxidized at 800°C was not related to an increased cell adhesion as has been reported [3, 15]. It has also been suggested that the highly polar (anionic) oxides formed by thermal oxidation on Ti alloys provides a more hydrophilic surface that attracts a variety of cations, which then bind electrostatically to proteins involved in cell adhesion (like fibronectin), thus enhancing cell attachment [3, 21]. In our study, the oxide surface formed on all the γ-TiAl surfaces had a similar composition, only varying in the concentration of certain oxides, as was described above. This finding can explain at least in part the lack of differences in cell adhesion between the autoclaved and the thermally oxidized γ-TiAl surfaces.

Although no differences were observed in cell adhesion on the different γ-TiAl surfaces, the hexosaminidase assay showed that osteoblast cells proliferated from day 1 to 7 on all the γ-TiAl surfaces, and that after this time the number of cells remained relatively constant. This was the expected

Fig. 5 hFOB 1.19 adhesion after 14-day culture as assessed by SEM on glass coverslips (**a**, **h**), GTi (**b**, **i**), GTi5 (**c**, **j**), GTi8 (**d**, **k**), TiV (**e**, **l**), TiV5 (**f**, **m**), and TiV8 (**g**, **n**) disks. Most samples exhibited osteoblasts with cell projections (*black arrow*), fibrous networks that may correspond to collagen (*black arrowhead*) and sponge-like structures that may correspond to mineral nodules (*white arrowheads*). On TiV8 only were observed structures that resemble cell debris (*white arrows*). Negative control surfaces (incubated with culture media for 14 days but without cells) corresponding to each surface are displayed in (**o**)–(**t**) panels. Magnification: **a**–**g** = ×1,500, **h**–**t** = ×5,000. Scale bar: *left* = 10 μm, *center* and *right* = 1 μm
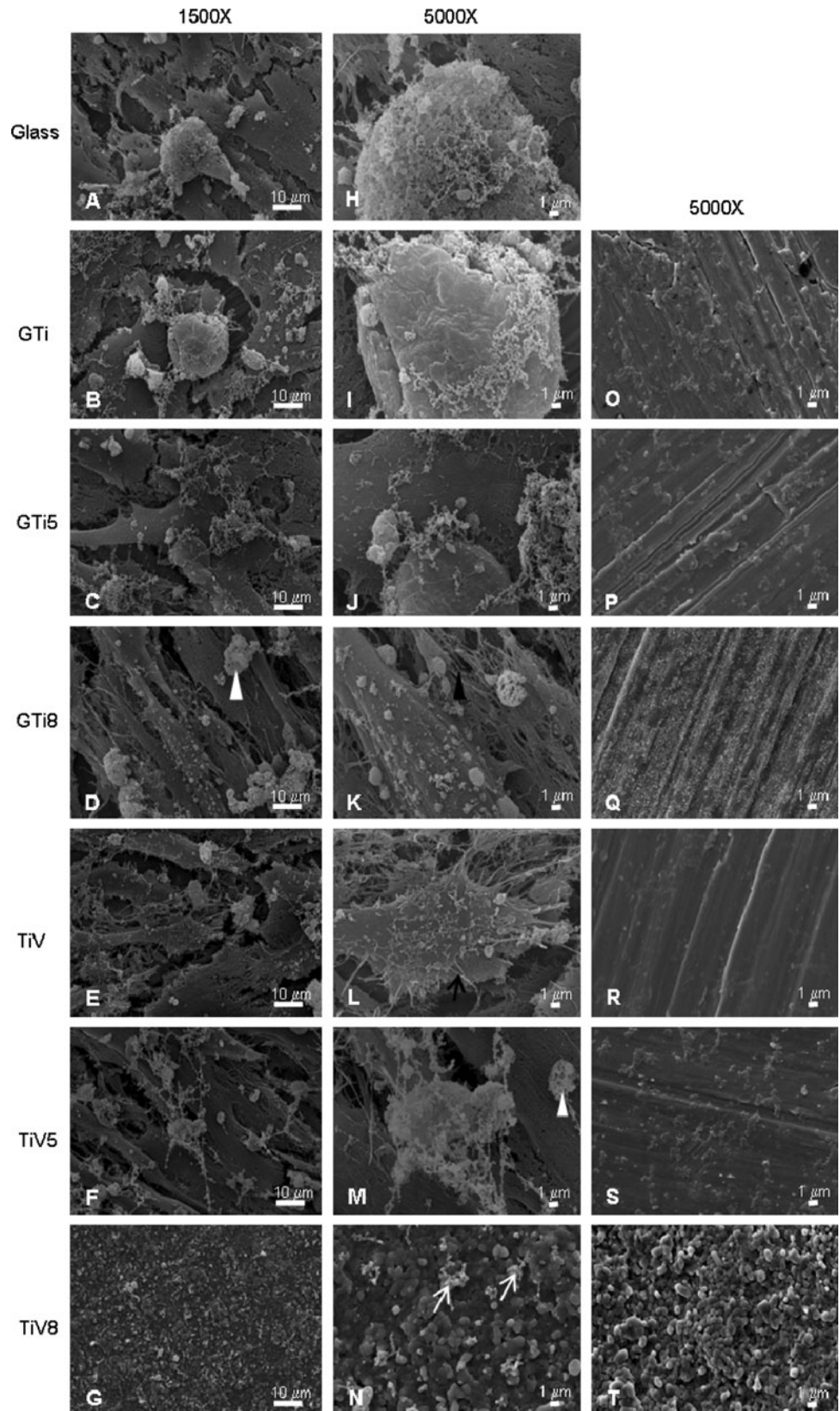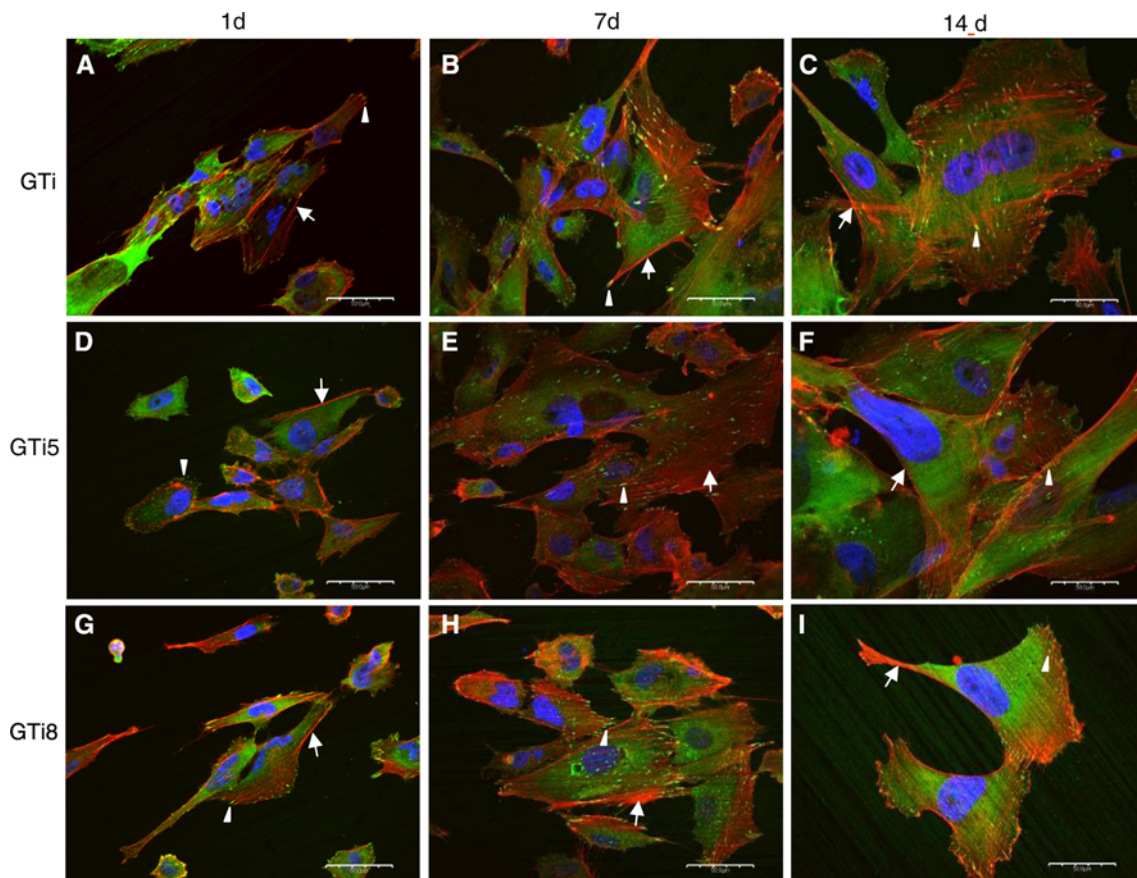
Fig. 6 Visualization by confocal laser scanning microscopy of focal adhesions and cytoskeleton of hFOB 1.19 cells after 1 day (**a**, **d**, **g**), 7 days (**b**, **e**, **h**), and 14 days (**c**, **f**, **i**) of seeding on autoclaved (**a–c**), thermally oxidized at 500°C (**d–f**)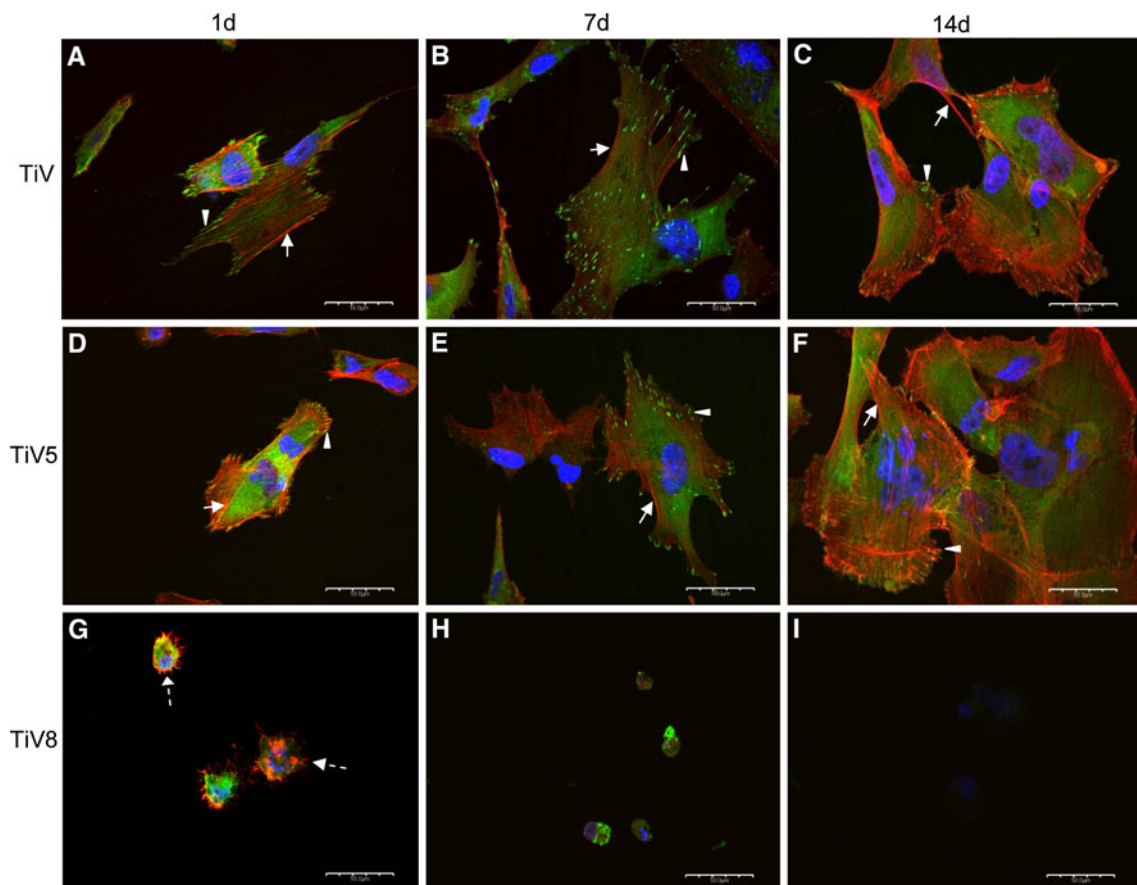, and at 800°C (**g–i**) γ-TiAl surfaces. Cells exhibited stress fibers (*arrows*), focal contacts at the cell periphery and at the end of the stress fibers (*arrowheads*). Scale bar: 50 μm

result since all the samples were incubated at a permissive temperature (33.5°C) until day 7, where hFOB 1.19 cells exhibit rapid cell division. On samples which were incubated at a restrictive temperature (39.5°C) from day 8 until day 14, hFOB 1.19 cell division is slowed down and differentiation increases [22, 23].

Immunofluorescent labeling of actin cytoskeleton showed that hFOB 1.19 cells adhered on all the γ-TiAl surfaces at day 1 exhibited stress fibers in a parallel arrangement and oriented in the direction of the long axis of the cells, which agrees with results previously published [24–26] for cells that are tightly adhered to implant materials. At this time point, most cells were elongated and polygonal which agree with the SEM observations. Similar cell characteristics were observed after 7 and 14 days; however, cells appeared more spread out compared to cells cultured for 1 day on all surfaces (Fig. 6i). A few focal adhesion contacts localized peripherally were observed in cells adhered on all the γ-TiAl surfaces at day 1 of culture, which could be associated with cell spreading [27]. An

increase in focal contacts over time (from day 1 to 7) was observed on all the γ-TiAl surfaces, which agrees with observations previously published [24]. At day 7, the focal contacts were scattered throughout the cell and located at the end of the stress fibers, which have been associated with a strong cell adhesion on smooth surfaces [28, 29], suggesting that in our experiment the contact between cells and all the γ-TiAl surfaces (independent of surface roughness) was stronger at day 7.

The number and size of focal contacts appear to decrease on all but autoclaved γ-TiAl surfaces after 14 days. The maintenance of cell adhesion when the osteoblasts become stable on substrates appears to be mediated by focal adhesions that are rich in focal adhesion kinase (FAK) but deficient in vinculin, which has been related to a decrease of vinculin-positive focal adhesions in a time dependent manner [24]. In this study, the decrease in the focal adhesions at day 14 may be due to the inhibition of vinculin expression when osteoblasts become stable on the thermally oxidized surfaces. Although Anselme et al.

Fig. 7 Visualization by confocal laser scanning microscopy of focal adhesions and cytoskeleton of hFOB 1.19 cells after 1 day (**a**, **d**, **g**), 7 days (**b**, **e**, **h**), and 14 days (**c**, **f**, **i**) of seeding on autoclaved (**a–c**), thermally oxidized at 500°C (**d–f**), and at 800°C (**g–i**) Ti–6Al–4V surfaces. Cells exhibited microspikes (*dashed arrows*), stress fibers (*arrows*), focal contacts at the cell periphery or at the end of the stress fibers (*arrowheads*). Scale bar: 50 μm

[28] did not observe differences in focal contact distribution with time in culture, they observed a decrease in the vinculin immunolabeling intensity after 14 days of culture.

The evaluation of cell adhesion by SEM showed hFOB 1.19 osteoblasts attached on all γ-TiAl surfaces forming confluent multilayers after 14 days of culture. Cells displayed the typical osteoblast morphology (elongated and polygonal) [30] on glass coverslips (positive control) as well as on the different γ-TiAl metallic surfaces evaluated. This finding suggests that surface oxides produced by thermal oxidation at 500 and 800°C on γ-TiAl did not induce alterations in hFOB 1.19 cell morphology. Osteoblasts grown on the γ-TiAl surfaces displayed various characteristics, such as dorsal vesicles, cellular extensions (filopodia), presence of nodules of mineralization and fibrous networks, which suggest its differentiation and the formation of a bone-like tissue at day 14 of culture.

hFOB 1.19 cell adhesion on autoclaved and Ti–6Al–4V thermally oxidized at 500°C surfaces was similar to that observed on γ-TiAl. However, the results of the hexosaminidase assay, the SEM and the immunofluorescent analyses of cell adhesion proteins indicate that the Ti–6Al–4V thermally oxidized at 800°C surface displays unexpectedly cytotoxic effects on hFOB 1.19 cells in a time dependent manner in contrast to the findings of García-Alonso et al. [13] and Saldaña et al. [14].

XPS data did not show significant differences in the composition of the oxide scales formed on autoclaved (TiV) and heat-treated at 500°C (TiV5) and 800°C (TiV8) Ti–6Al–4V alloys. TiO_2, Al_2O_3, and V_2O_5/VO_2 oxides were present on both thermally oxidized surfaces, which agrees with data in literature [3, 13, 17, 18]. However, the V/Ti ratio on TiV8 was higher than the same ratio on TiV5 suggesting that oxidation at 800°C causes an enrichment of V oxides on TiV8, which could be associated with the cytotoxicity.

The deleterious effects of the V_2O_5 produced by thermal oxidation of the high V content Ti alloy Ti–1.5Al–25V on MC3T3-murine osteoblasts and vero-fibroblasts cells were demonstrated in vitro [31]. The vero cells cultured for 7 days on the thermally oxidized Ti–1.5Al–25V surfaces, which were rich in V_2O_5, showed a decreased proliferation

and viability (determined by MTT) compared to cells cultured on the reference surface (cp-Ti). Additionally, vero fibroblasts showed a decreased cytoplasm content that exhibited vacuoles. These cells were also much smaller and the length and number of the cell branches were decreased compared to cells cultured on cp-Ti surfaces. MC3T3-murine osteoblasts cultured for 7 days on the same thermally oxidized high V content Ti alloy displayed scarce stress fibers which were poorly organized, indicating a weaker adhesion to the thermally oxidized surface compared to the reference surface.

In this study, some of the cytotoxic effects reported for the V_2O_5 on the MC3T3-osteoblasts and the vero-fibroblasts were also observed on the hFOB 1.19 cells cultured for the different time points tested on the thermally oxidized Ti–6Al–4V surfaces at 800°C (TiV8). These also appeared enriched with V oxides (V_2O_5/VO_2), as indicated by the XPS studies. A few hFOB 1.19 cells were adhered on TiV8 surfaces at day 1 but they did not proliferate as indicated by the hexosaminidase assay. CLSM studies showed that hFOB cells after 7 days of incubation on TiV8 were rounded and smaller compared to hFOB 1.19 cells cultured on the other surfaces tested. At this time point, hFOB 1.19 cells did not display neither stress fibers nor focal contacts. MacDonald et al. [3] found VO_2 and V_2O_5 on Ti–6Al–4V thermally oxidized surface (600°C, 1 h), but these oxide layers did not affect the MG63 cell attachment [3], this likely due to the short time (2 h) of contact of cells on the thermally oxidized Ti–6Al–4V surface. In this study, SEM and CLSM studies showed only cell remnants at day 14 post-seeding, indicating that the cytotoxic effects of the V oxides are time-dependent.

The TiV8 surface oxide exhibits a porous structure, which may be responsible for the lower corrosion resistance of this surface in Ringer's solution compared to TiV and TiV5 surfaces [5]. Accelerated oxidation rate of Ti–6Al–4V has been associated with the formation of a defective oxide layer where microcracks and micropores are observed, whereas oxides with fewer defects are formed at low temperatures after longer oxidation times [8]. The oxide layers with structural defects gradually detach from the surface as fragments because the whole oxide layer is in stress [8]. In this study, the oxide layer formed on TiV8 was the only surface that was partially detached in culture conditions, suggesting that this oxide layer had structural defects and was in stress due to the accelerated oxidation rate of formation. Thus the slow and continuous release of harmful ions from the bulk alloy (Ti–6Al–4V) to the surface through the pores/microcracks/micropores of oxide layer, which could act as easy diffusion paths toward the surface, remains as a possible explanation for the lack or the small number of osteoblasts adhered on TiV8 at 7 and 14 days postseeding.

Additionally, it has been suggested that Al and V may exist as ions at interstitial or substitutional sites in the Ti oxide matrix formed on thermally oxidized Ti–6Al–4V [18]. Thus, more Al and V ions could be trapped during the oxidation process in the porous structure of the oxide layer on TiV8, and such ions could be easily released through the pores to the surface. Currently, our group is performing cytotoxic studies in an attempt to identify the cause of the deleterious effects on the hFOB 1.19 cells of the V-rich oxide surfaces observed on Ti–Al–4V by thermal oxidation.

Although the in vitro evaluation of the osteoblast adhesion on thermally oxidized γ-TiAl surfaces oxidized at 500 and 800°C indicate that both surfaces are biocompatible and hence have the potential for enhancing the use of γ-TiAl as an implant material, further studies to determine the gene-expression response to thermally oxidized γ-TiAl surfaces could give some useful insights about the ability of osteoblasts to differentiate on thermally oxidized γ-TiAl surfaces. The composition of the ECM secreted on the thermally oxidized γ-TiAl surfaces by the osteoblast cells must be determined to predict the osseointegration capability of the oxidized γ-TiAl surfaces. Finally, in vivo studies must be performed to determine the response of osteoblast cells to the thermally oxidized γ-TiAl surfaces in a biological environment.

5 Conclusions

In this study, thermal treatment (500 or 800°C for 1 h) of the potential biomaterial Ti–48Al–2Cr–2Nb was shown to generate oxide layers that allow the adhesion and proliferation of hFOB 1.19 cells in a manner similar to oxide layers generated on γ-TiAl by autoclaving. Cell adhesion on autoclaved and Ti–6Al–4V disks thermally oxidized at 500°C was similar to cell attachment on both oxidized and autoclaved γ-TiAl disks. Nevertheless, fewer cells were attached to Ti–6Al–4V disks oxidized at 800°C compared to the other surfaces evaluated, suggesting that this surface does not allow cell proliferation and has toxic effects on hFOB 1.19 cells. Taken together, these findings suggest that thermally oxidized γ-TiAl appears to be biocompatible and that this material can be recommended for further preclinical and clinical research.

for the technical assistance with the laser confocal and scanning electron microscopy.

References

1. Khan MA, Williams RL, Williams DF. The corrosion behaviour of Ti–6Al–4V, Ti–6Al–7Nb and Ti–13Nb–13Zr in protein solutions. Biomaterials. 1999;20:631–7.
2. Li J, Sun M, Ma X, Tang G. Structure and tribological performance of modified layer on Ti6Al4V alloy by plasma-based ion implantation with oxygen. Wear. 2006;261:1247–52.
3. MacDonald DE, Rapuano BE, Deo N, Stranick M, Somasundaran P, Boskey AL. Thermal and chemical modification of titanium–aluminum–vanadium implant materials: effects on surface properties, glycoprotein adsorption, and MG63 cell attachment. Biomaterials. 2004;25:3135–46.
4. Escudero ML, Muñoz-Morris MA, García-Alonso MC, Fernández-Escalante E. In vitro evaluation of a γ-TiAl intermetallic for potential endoprothesic applications. Intermetallics. 2004;12:253–60.
5. Delgado-Alvarado C, Sundaram PA. Corrosion evaluation of Ti–48Al–2Cr–2Nb (at.%) in Ringer's solution. Acta Biomater. 2006;2:701–8.
6. Rivera-Denizard O, Diffoot-Carlo N, Navas V, Sundaram PA. Biocompatibility studies of human fetal osteoblast cells cultured on gamma titanium aluminide. J Mater Sci Mater Med. 2008;19:153–8.
7. Castañeda-Muñoz DF, Sundaram PA, Ramírez N. Bone tissue reaction to Ti–48Al–2Cr–2Nb (at.%) in a rodent model: a preliminary SEM study. J Mater Sci Mater Med. 2007;18:1433–8.
8. Guleryuz H, Cimenoglu H. Effect of thermal oxidation on corrosion and corrosion-wear behaviour of a Ti–6Al–4V alloy. Biomaterials. 2004;25:3325–33.
9. Hanawa T. In vivo metallic biomaterials and surface modification. Mater Sci Eng. 1999;267A:260–6.
10. Thompson GJ, Puleo DA. Ti–6Al–4V ion solution inhibition of osteogenic cell phenotype as a function of differentiation timecourse in vitro. Biomaterials. 1996;17:1949–54.
11. Jacobs JJ, Hallab NJ, Urban RM, Wimmer MA. Wear particles. J Bone Joint Surg Am. 2006;88A:99–102.
12. Chung SH, Heo SJ, Koak JY, Kim SK, Lee JB, Han JS, et al. Effects of implant geometry and surface treatment on osseointegration after functional loading: a dog study. J Oral Rehabil. 2008;35:229–36.
13. García-Alonso MC, Saldaña L, Vallés G, González-Carrasco JL, González-Cabrero J, Martínez ME, et al. In vitro corrosion behaviour and osteoblast response to thermally oxidized Ti6Al4V alloy. Biomaterials. 2003;24:19–26.
14. Saldaña L, Vilaboa N, Vallés G, González-Cabrero J, Munuera L. Osteoblast response to thermally oxidized Ti6Al4V alloy. J Biomed Mater Res. 2005;73A:97–107.
15. Saldaña L, Barranco V, González-Carrasco JL, Rodríguez M, Munuera L, Vilaboa N. Thermal oxidation enhances early interactions between human osteoblasts and alumina blasted Ti6Al4V alloy. J Biomed Mater Res. 2007;81A:334–46.
16. Landegren U. Measurement of cell numbers by means of the endogenous enzyme hexosaminidase. Applications to detection of lymphokines and cell surface antigens. J Immunol Methods. 1984;67:379–88.
17. Milosev I, Metikos-Hukovic M, Strehblow HH. Passive film on orthopaedic TiAlV alloy formed in physiological solution investigated by X-ray photoelectron spectroscopy. Biomaterials. 2000;21:2103–13.
18. Shodi RNS, Weninger A, Davies JE. X-ray photoelectron spectroscopy comparison of sputtered Ti, Ti6Al4V, and passivated bulk metals for use in cellular culture techniques. J Vac Sci Technol A. 1991;9:1329–33.
19. Kern T, Yang Y, Glover R, Ong JL. Effect of heat-treated titanium surfaces on protein adsorption and osteoblast precursor cell line initial attachment. Implant Dent. 2005;14:70–6.
20. Feng B, Weng J, Yang BC, Qu SX, Zhang XD. Characterization of surface oxide films on titanium and adhesion of osteoblast. Biomaterials. 2003;24:4663–70.
21. Bess E, Cavin R, Ma K, Ong JL. Protein adsorption and osteoblast responses to heat-treated titanium surfaces. Implant Dent. 1999;8:126–32.
22. Harris SA, Enger R, Riggs L, Spelberg T. Development and characterization of a conditionally immortalized human fetal osteoblastic cell line. J Bone Miner Res. 1995;10:178–86.
23. Subramaniam M, Jalal SM, Rickard DJ, Harris SA, Bolander ME, Spelsberg TC. Further characterization of human fetal osteoblastic hFOB 1.19 and hFOB/ERα cells: bone formation in vivo and karyotype analysis using multicolor fluorescent in situ hybridization. J Cell Biochem. 2002;87:9–15.
24. Okamura A, Goto M, Goto T, Yoshinari M, Masuko S, Katsuki T, et al. Substrate affects the initial attachment and subsequent behavior of human osteoblastic cells (Saos-2). Biomaterials. 2001;22:2263–71.
25. Yang XF, Chen Y, Yang F, He FM, Zhao SF. Enhanced initial adhesion of osteoblast-like cells on an anatase-structured titania surface formed by H2O2/HCl solution and heat treatment. Dent Mater. 2009;25:473–80.
26. Setzer B, Bachle M, Metzger M, Kohal R. The gene-expression and phenotypic response of hFOB 1.19 osteoblasts to surface-modified titanium and zirconia. Biomaterials. 2009;30:979–90.
27. Beningo KA, Dembo M, Kaverina I, Small JV, Wang Y. Nascent focal adhesions are responsible for the generation of strong propulsive forces in migrating fibroblasts. J Cell Biol. 2001;153:881–7.
28. Anselme K, Bigerelle M, Noel B, Dufresne E, Judas D, Iost A, et al. Qualitative and quantitative study of human osteoblast adhesion on materials with various surface roughnesses. J Biomed Mater Res. 2000;49:155–66.
29. Linez-Bataillon P, Monchau F, Bigerelle M, Hildebrand HF. In vitro MC3T3 osteoblast adhesion with respect to surface roughness of Ti–6Al–4V substrates. Biomol Eng. 2002;19:133–41.
30. Schmidt C, Kaspar D, Sarkar MR, Claes LE, Ignatius AA. A scanning electron microscopy study of human osteoblast morphology on five orthopedic metals. J Biomed Mater Res. 2002;63B:252–61.
31. Eisenbarth E, Velten D, Schenk-Meuser K, Linez P, Biehl V, Dushner H, et al. Interactions between cells and titanium surfaces. Biomol Eng. 2002;19:243–9.